THE MAXIMUM LIFT COEFFICIENT OF PLAIN WINGS AT SUBSONIC SPEEDS

1. NOTATION AND UNITS

		SI	*British*
A	aspect ratio ($= 2s/\bar{c}$)		
C_L	lift coefficient, lift/qS		
C_{L0}	section lift coefficient at zero incidence		
C_{LL}	local lift coefficient		
C_{LLp}	peak local lift coefficient, see Sketch 6.1		
C_{Lmax}	wing maximum lift coefficient		
C_{Lm}	aerofoil section maximum lift coefficient at $M \approx 0$		
ΔC_{LM}	increment in wing maximum lift coefficient due to Mach number		
ΔC_{LR}	increment in wing maximum lift coefficient due to Reynolds number for $\Lambda_0 > 37°$		
ΔC_{LT}	increment in wing maximum lift coefficient due to twist		
$\Delta C_{L\Lambda}$	increment in wing maximum lift coefficient dependent on leading-edge sweep and ζ_p		
c	local chord	m	ft
$\bar{c}$	geometric mean chord	m	ft
$\bar{\bar{c}}$	aerodynamic mean chord	m	ft
c_r	wing root chord	m	ft
c_t	wing tip chord	m	ft
M	free-stream Mach number		
q	free-stream kinetic pressure	N/m^2	lbf/ft^2
R_c	Reynolds number based on local chord and free-stream velocity		
$R_{\bar{\bar{c}}}$	Reynolds number based on aerodynamic mean chord and free-stream velocity		

Issued October 1989
With Amendment A, August 1993

S	wing area, $s(c_r + c_t)$	m^2	ft^2
s	wing semispan	m	ft
x	general chordwise station measured streamwise from wing leading edge, see Sketch 1.2	m	ft
x_{um}	chordwise station for z_{um} , see Sketch 1.1	m	ft
z	general section ordinate	m	ft
z_{um}	maximum upper-surface ordinate, see Sketch 1.1	m	ft
$z_{u1.25}$	upper-surface ordinate at 1.25% chord, see Sketch 1.1	m	ft
α_0	zero-lift angle of incidence for cambered two-dimensional section	degree	degree
β	compressibility parameter, $(1 - M^2)^{½}$		
δ	wing twist angle relative to wing root (positive leading edge up)	degree	degree
δ_e	effective twist angle	degree	degree
δ_{et}	effective tip twist angle	degree	degree
ζ_p	leading-edge shape parameter, $(z_{u1.25}/c)_p \sec\Lambda_0$		
η	spanwise distance from wing root as fraction of semispan		
η_p	value of η for μ_p		
$\bar{\eta}$	spanwise centre of pressure position, $\int_0^1 \sigma\eta \, d\eta$		
κ	wing taper parameter, $\int_0^1 (c/\bar{c})\eta \, d\eta$		
Λ_0	wing leading-edge sweep angle	degree	degree
$\Lambda_{¼}$	wing quarter-chord sweep angle	degree	degree
$\Lambda_{½}$	wing mid-chord sweep angle	degree	degree
Λ_1	wing trailing-edge sweep angle	degree	degree
λ	wing taper ratio, c_t/c_r		
μ	normalised local lift coefficient, C_{LL}/C_L		
μ_p	peak value of μ		

σ	spanwise loading due to incidence, $C_{LL}c/C_L\bar{c}$		
τ_u	aerofoil upper-surface angle defined by Equation (6.2), see also Sketch 1.1	degree	degree

Subscripts

$( )_{expt}$	denotes experimental value
p	denotes value for section at η_p
$( )_{pred}$	denotes predicted value
r	denotes value for section at wing root
t	denotes value for section at wing tip
η	denotes values for section at η

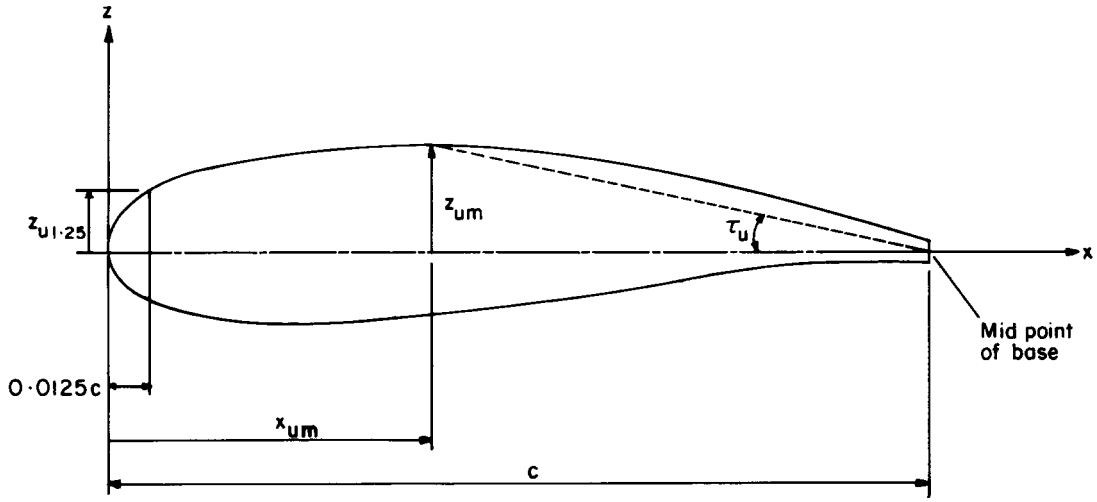

Sketch 1.1 Aerofoil geometry

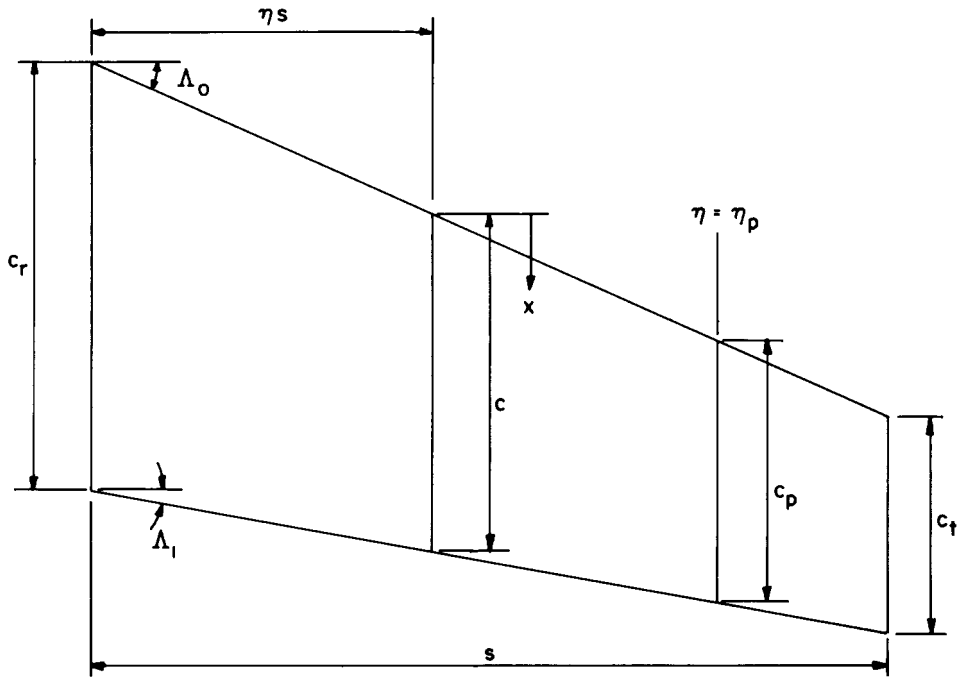

Sketch 1.2 Wing notation

2. INTRODUCTION

Item No. 84026 (Derivation 5) provides a method for the prediction of maximum lift of aerofoil sections. This Item extends the scope of Item No. 84026 to apply to "plain" wings with or without camber or twist. Here, "plain" means without deflection of manoeuvre or high-lift devices such as leading-edge and trailing-edge flaps.

For subsonic speeds, the maximum lift of high aspect ratio wings is, to a first approximation, determined by the maximum lift of the aerofoil section. The main parameters which influence the maximum lift coefficient for an aerofoil section are section geometry, including camber, surface condition (*i.e.* smooth or rough), Reynolds number and Mach number. For wings, additional parameters influence the maximum lift coefficient, in particular aspect ratio, taper ratio, sweep, twist and spanwise variation of aerofoil section.

Because of three-dimensional effects, separation usually starts near the most highly loaded spanwise station and spreads rapidly with increasing incidence. For highly tapered wings separation tends to be initiated at the tip, whilst for untapered wings separation tends to be initiated at the root. For swept wings, the induced effects combine to promote tip stall. This results from the high induced incidence and negative induced camber at the tip and the spanwise pressure gradient which tends to draw the boundary layer from the root to the tip. Regardless of the spanwise location where separation first appears, the maximum lift is greatly influenced by whether separation occurs at the leading edge or trailing edge.

Trailing-edge separation, a characteristic of thick wings, normally results in a loss of maximum lift as compared with that of an aerofoil section. Leading-edge separation, where for swept wings the flow rolls up to form a spanwise vortex, results in an increase in maximum lift, the magnitude of which is related to the strength of the vortex. The strength of this leading-edge vortex is dependent on aspect ratio, sweep, incidence and the section shape near the leading edge.

As aspect ratio decreases the wing planform parameters become increasingly important, with leading-edge vortex effects becoming more dominant.

3. REQUIRED DATA ITEMS

Other ESDU Data Items that may be required in the use of this Item are:

Derivation No.	Data Item No.	For determination of
1.	Aero W.01.01.05	Slope of lift curve for two-dimensional flow, for use in Derivation 5.
2.	66034	Upper-surface ordinate at 1.25% chord.
3.	76003	Various geometrical relationships for wings, and equivalent straight-tapered planform.
4.	83040	Spanwise centre of pressure position, $\bar{\eta}$.
5.	84026	Aerofoil maximum lift coefficient for $M \approx 0$.
6.	88030	Boundaries of linear characteristics of cambered and twisted wings at subcritical Mach numbers.

4. MAXIMUM LIFT AND MAXIMUM USABLE LIFT

In making use of the data derived from this Item it is essential to distinguish between wing maximum lift and wing maximum usable lift. The lift of the wing alone, as derived here, may be significantly modified by the presence of interference effects due to fuselages, nacelles, pylons, flap track fairings or other external additions to the configuration. Moreover, maximum usable lift may be limited by other effects associated with flow separation, such as pitch-up, buffet, or wing rock. For example, prior to the attainment of maximum lift it is often the case that the pitching moment curve is characterised by a pitch break, resulting in what can be a very marked and unacceptable change in longitudinal stability. Derivations 9 and 34 indicate configuration parameters which will result in acceptable pitch characteristics. It may be noted that some improvement can be obtained by the use of leading-edge devices. Also, acceptable behaviour may result for configurations outside those guidelines, provided that the aircraft tailplane is properly positioned or adequate control effectiveness is provided.

In this Item C_{Lmax} is taken as the greatest value achieved irrespective of the pitching moment characteristics prior to the maximum value of lift. It may be noted that for some wing-body configurations at all Mach numbers, and for wings or wing-body combinations at high subsonic Mach numbers where shock separation affects the development of the stall, a first peak or plateau in C_L is often followed by a subsequent recovery to greater values. None of the data analysed for wings alone exhibited this characteristic within the range of Mach number and planform and section parameters covered by this Item.

5. EFFECTS OF MACH NUMBER AND REYNOLDS NUMBER

5.1 Mach Number Effects

In the preparation of this Item it was found that the effect of Mach number on the maximum lift coefficient for wings can be very different from that shown for two-dimensional sections in Item No. 84026. For this Item the effect has been correlated as an increment, $\Delta C_{LM}/\cos^4\Lambda_0$, dependent on $M\cos\Lambda_0$ and on ζ_p, the value of $(z_{u1.25}/c)$ sec Λ_0 for the most highly loaded section, η_p.

5.2 Reynolds Number Effects

For wings with leading-edge sweep angles up to about 37 degrees the effect of Reynolds number is adequately estimated by the use of the two-dimensional section data of Item No. 84026. For wings with greater leading-edge sweep the effect of Reynolds number on maximum lift coefficient is greatly reduced. From correlations of the data used in the preparation of this Item it was found that there was a systematic trend with sweep, independent of leading-edge sectional geometry. The increment in maximum lift coefficient, ΔC_{LR}, has been correlated as a function of Λ_0 and $R_{cp}\cos^2\Lambda_0$, which can be regarded as the local Reynolds number of the flow normal to the leading edge at η_p.

6. PREDICTION METHOD

6.1 Derivation of Method

The method is developed from that of Derivations 7, 8, 36, 37 and 39. For wings with little or no sweep, where the effects of outboard flow of the boundary layer may be neglected, it is necessary to establish the spanwise variation of C_{LL} and to compare this with the spanwise variation of C_{Lm}, the maximum lift coefficient for the aerofoil section. To obtain the spanwise lift distribution at this condition, calculations including the effects of camber and twist may be made using (for example) Item No. 83040 for a number of incidences. For the incidence at which the peak local lift coefficient, C_{LLp}, matches the local section maximum lift coefficient, C_{Lm}, the distribution of $C_{LL}c/\bar{c}$ must be obtained and integrated to obtain the value of the maximum lift coefficient for the wing, C_{Lmax}, see Sketch 6.1.

To derive the method of this Item, the same simplifying assumptions as those used in Item No. 88030 have been made to reduce the relatively complex procedure outlined above to the calculation for only the most highly loaded spanwise station. The spanwise position, η_p, of the most highly loaded section for the loading due to incidence and the corresponding maximum normalised lift coefficient, μ_p, are shown in Figures 1 and 2, which are taken from Item No. 88030. These Figures are in terms of taper ratio, λ, and the spanwise centre of pressure position, $\bar{\eta}$, corresponding to the spanwise loading due to incidence, obtainable from Item No. 83040.

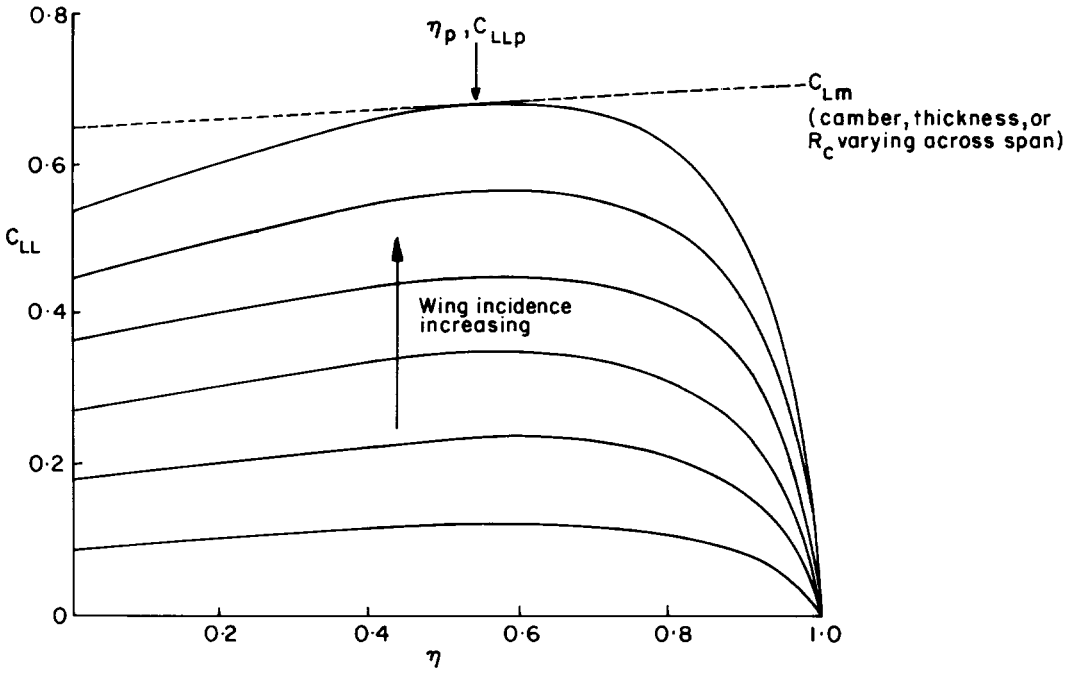

Sketch 6.1

For large amounts of twist or large variation of C_{Lm} across the span due to exceptionally rapid changes of camber or a section characteristic critically dependent on Reynolds number the method of this Item may not give reliable results. However, for the usual case where these variations are more gradual the method of this Item may be used with confidence.

6.2 Unswept, Untwisted Wings

For an untwisted wing with little or no sweep ($\Lambda_0 \leq 10°$, say) the maximum lift coefficient is given by:

$$C_{Lmax} = C_{Lm}/\mu_p + \Delta C_{LM} \tag{6.1}$$

where C_{Lm} is the value of maximum lift coefficient at $M \approx 0$ for the aerofoil section at η_p and may be obtained from Item No. 84026. The parameter ΔC_{LM} is the increment on wing maximum lift coefficient due to Mach number (see Section 6.3).

The spanwise position of the most highly loaded section, η_p, may be obtained from Figure 1 as a function of taper ratio, λ, and spanwise centre of pressure position, $\bar{\eta}$. The parameter $\bar{\eta}$ may be obtained from Item No. 83040 (Derivation 4) as a function of the planform parameters, reduced wing aspect ratio, βA, a wing taper parameter, κ, and mid-chord sweep parameter, $A\tan\Lambda_{1/2}$.

The ratio of the peak local lift coefficient to the wing lift coefficient, $C_{LLp}/C_L (= \mu_P)$, for the loading due to incidence may be obtained from Figure 2 as a function of λ and $\bar{\eta}$.

It should be noted that the value of C_{Lm} from Item No. 84026 is dependent on camber, Reynolds number, R_c, and $z_{u1.25}/c$. Moreover, in cases of a trailing-edge stall, identified when $z_{u1.25}/c > 0.017$, C_{Lm} also depends on $\tan\tau_u$. The quantity τ_u is the angle between the chord line and a line drawn from the maximum

upper-surface ordinate to the trailing-edge point (see Sketch 1.1) given by

$$\tan\tau_u = (z_{um}/c)/(1 - x_{um}/c) \tag{6.2}$$

6.3 Swept, Untwisted Wings

For an untwisted swept wing the maximum lift coefficient is given by:

$$C_{Lmax} = C_{Lm}/\mu_p + \Delta C_{LM} + \Delta C_{LR} + \Delta C_{L\Lambda} \tag{6.3}$$

where C_{Lm} is obtained as described below and μ_p is obtained as described in Section 6.2,

ΔC_{LM} is obtained from Figure 3 which gives $\Delta C_{LM}/\cos^4\Lambda_0$ as a function of $M\cos\Lambda_0$ and ζ_p,

ΔC_{LR} is obtained from Figure 4 and is dependent on Λ_0 and $R_{cp}\cos^2\Lambda_0$

and $\Delta C_{L\Lambda}$ is obtained from Figure 5 and is dependent on Λ_0 and ζ_p.

Values of $R_{cp}\cos^2\Lambda_0$, ζ_p, $\tan\tau_u\sec\Lambda_1$ and $C_{L0}\sec\Lambda_0$ are used in place of R_c, $z_{u1.25}/c$, $\tan\tau_u$ and C_{L0} respectively to obtain C_{Lm} at $M \approx 0$ from Item No. 84026. Such considerations do not, of course, apply to the determination of C_{L0} itself.

Figure 5 is subdivided into 5a and 5b which correspond roughly to leading-edge separation and trailing-edge separation respectively.

6.4 Twisted Wings

6.4.1 Increment in maximum lift coefficient due to twist

The effect of twist on maximum lift coefficient has been found to agree well with the effect of twist on the lift coefficient for the end of the initial linear range of force and moment characteristics presented in Item No. 88030 (Derivation 6). The method is described for a wing with linear twist. For cases where the twist is monotonic, but not excessively non-linear (a tapered wing with linear-lofted twist for example), it is recommended that an equivalent linear twist be assumed in which the tip twist δ_t is taken to be 3/2 times the twist angle δ at $\eta = 2/3$.

If the camber is not uniform, it is necessary to use a combined, or effective, twist in place of δ, *i.e.*

$$\delta_e = \delta_\eta + \alpha_{0r} - \alpha_{0\eta}, \tag{6.4}$$

and hence, in place of δ_t,

$$\delta_{et} = \delta_t + \alpha_{0r} - \alpha_{0t}, \tag{6.5}$$

or with the necessary modification to allow for minor non-linearity

$$\delta_{et} = 3(\delta_{2/3} + \alpha_{0r} - \alpha_{02/3})/2. \tag{6.6}$$

In these expressions α_{0r}, $\alpha_{02/3}$, and α_{0t} are the zero-lift angles for the streamwise sections at the root

station, $\eta = 2/3$, and the tip station respectively and may be obtained by the method in Section 5 of Item No. 84026.

Figure 6 presents values of the increment in maximum lift coefficient for unit δ_{et}, $\Delta C_{LT}/\delta_{et}$, taken from Item No. 88030 for wings with linear twist. These carpets require interpolation in A, λ and $\tan\Lambda_{½}$. The increment is therefore obtained from

$$\Delta C_{LT} = (\Delta C_{LT}/\delta_{et})\delta_{et}. \tag{6.7}$$

6.4.2 Unswept wings with twist

For a twisted wing with little or no sweep ($\Lambda_0 \leq 10°$, say) the maximum lift coefficient is given by

$$C_{Lmax} = C_{Lm}/\mu_p + \Delta C_{LM} + \Delta C_{LT}, \tag{6.8}$$

where C_{Lm}/μ_p it is obtained as described in Section 6.2, and ΔC_{LM} and ΔC_{LT} are obtained as described in Sections 6.3 and 6.4.1 respectively.

6.4.3 Swept wings with twist

For a twisted swept wing the maximum lift coefficient is given by

$$C_{Lmax} = C_{Lm}/\mu_p + \Delta C_{LM} + \Delta C_{LR} + \Delta C_{L\Lambda} + \Delta C_{LT}, \tag{6.9}$$

where C_{Lm}/μ_p, ΔC_{LM}, ΔC_{LR} and $\Delta C_{L\Lambda}$ are obtained as described in Section 6.3 and ΔC_{LT} is obtained as described in Section 6.4.1.

7. APPLICABILITY AND ACCURACY

7.1 Applicability

The method given in this Item for estimating the maximum lift of plain wings is applicable to straight-tapered wings with or without camber and twist provided that the local effective twist is not excessive ($\delta_{et} < 10°$ say). The method can cope with any shape of section or camber line, both of which may vary across the span. Although the method is presented for a linear spanwise variation of combined twist, incorporating spanwise twist and variation of camber, it may be used for wings with non-linear monotonic variation of twist by assuming an equivalent linear twist. The method is restricted to wings with smooth surfaces or with a narrow band of roughness with height just sufficient to ensure boundary-layer transition. It should be noted that a very rough leading edge can result in a large reduction in the maximum lift coefficient. Item No. 84026 shows the effect of roughness on the maximum lift coefficient for an aerofoil section.

For wings with leading-edge sweep angle, Λ_0, up to about 10º the method described in Sections 6.2 and 6.4.2 for unswept wings provides reliable results. For wings with $\Lambda_0 > 10°$ the method described in Sections 6.3 and 6.4.3 for swept wings should be used. The only data available with a swept-forward wing, which had 43° of leading-edge sweep and an aspect ratio of 4, gave good correlation, but the method should not be relied on for swept-forward wings.

For wings with cranked or curved leading or trailing edges it is suggested that the calculation of maximum lift coefficient be made for the equivalent straight-tapered planform as defined in Item No. 76003.

The wind-tunnel data used in the development of this Item covered the following ranges of parameters.

TABLE 7.1

Parameter	*Range*
Taper ratio, λ	0.20 to 1.0
Aspect ration, A	2 to 12
Leading-edge sweep, Λ_0	0 to 50°
Trailing-edge sweep, Λ_1	0 to 45°
$M\cos\Lambda_0$	0 to 0.6
$R_{cp}\cos^2\Lambda_0$	0.3 to 10 × 10^6
Reynolds number, $R_{\bar{c}}$	0.7 to 12 × 10^6
Mach number, M	0 to 0.8

7.2 Accuracy

7.2.1 Unswept wings

Sketch 7.1 shows the correlation of data for C_{Lmax} for cambered and uncambered wings having sections with leading-edge and trailing-edge separation types and leading-edge sweep from 0 to 10° (from Derivations 10, 13, 18, 19, 20, 26, 27, 29, 30, 31, 33 and 35). All the data for aspect ratios within the range of applicability shown in Table 7.1 are predicted to within about ±10% . The method is recommended for general use down to an aspect ratio of 2.0. However, it has been found that for wings with no taper or sweep satisfactory agreement is obtained down to A = 1.0 as shown in Sketch 7.1.

7.2.2 Swept wings

Sketches 7.2 and 7.3 show the correlation of data for C_{Lmax} for cambered and uncambered wings having sections with leading-edge and trailing-edge separation types. Sketch 7.2 is for wings with $10° < \Lambda_0 \leq 40°$ (from Derivations 7, 12, 13, 15, 16, 17, 19, 22, 27, 28, 33, 35 and 40) and Sketch 7.3 is for wings with $40° < \Lambda_0 < 50°$ (from Derivations 11, 13, 14, 18, 19, 21, 23, 24, 25, 27, 32, 35, 38 and 40) respectively. The values of C_{Lmax} are predicted to within ±10% for 95% of the data.

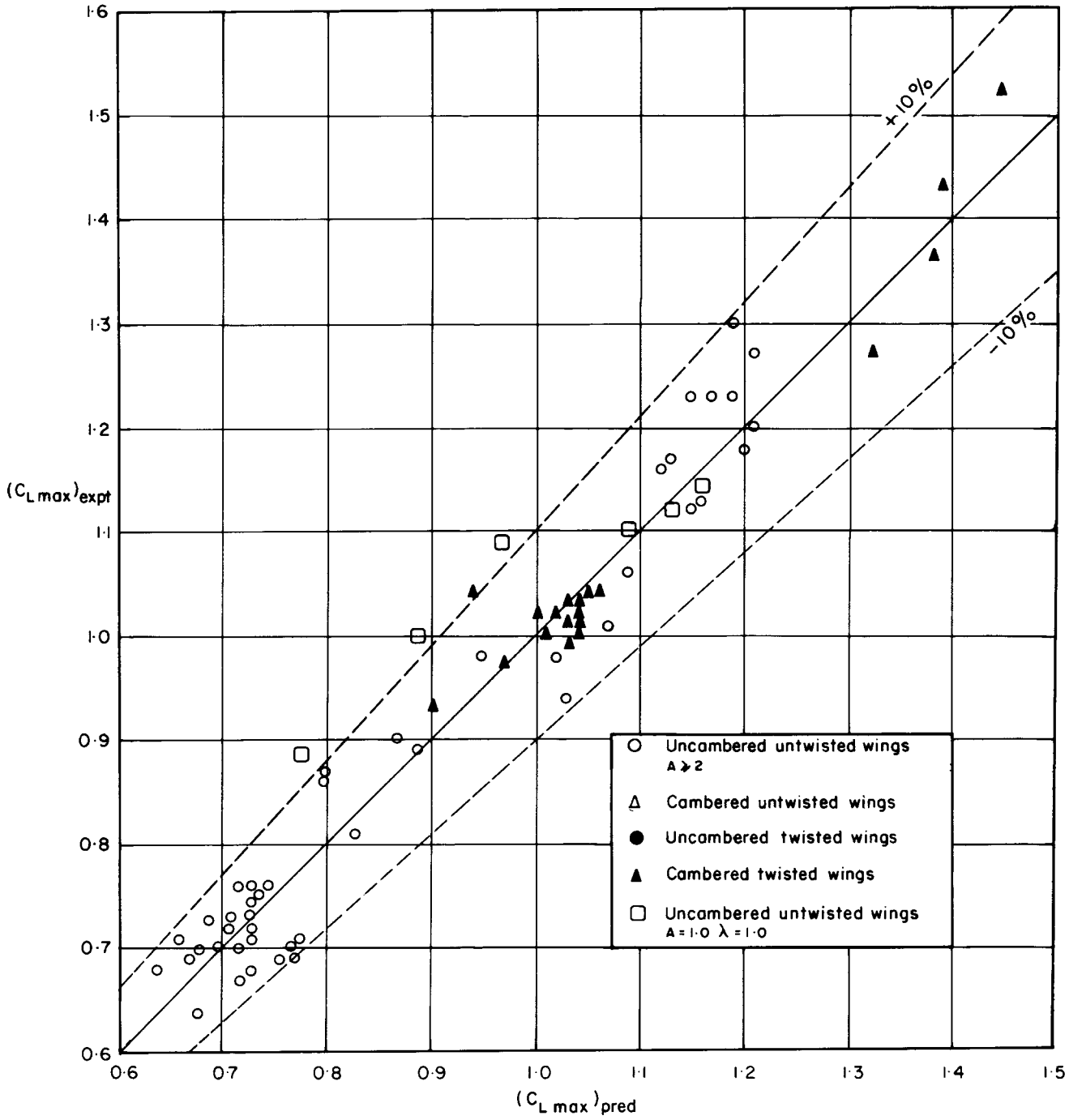

Sketch 7.1 Correlation for unswept wings $0 < \Lambda_0 \leq 10°$

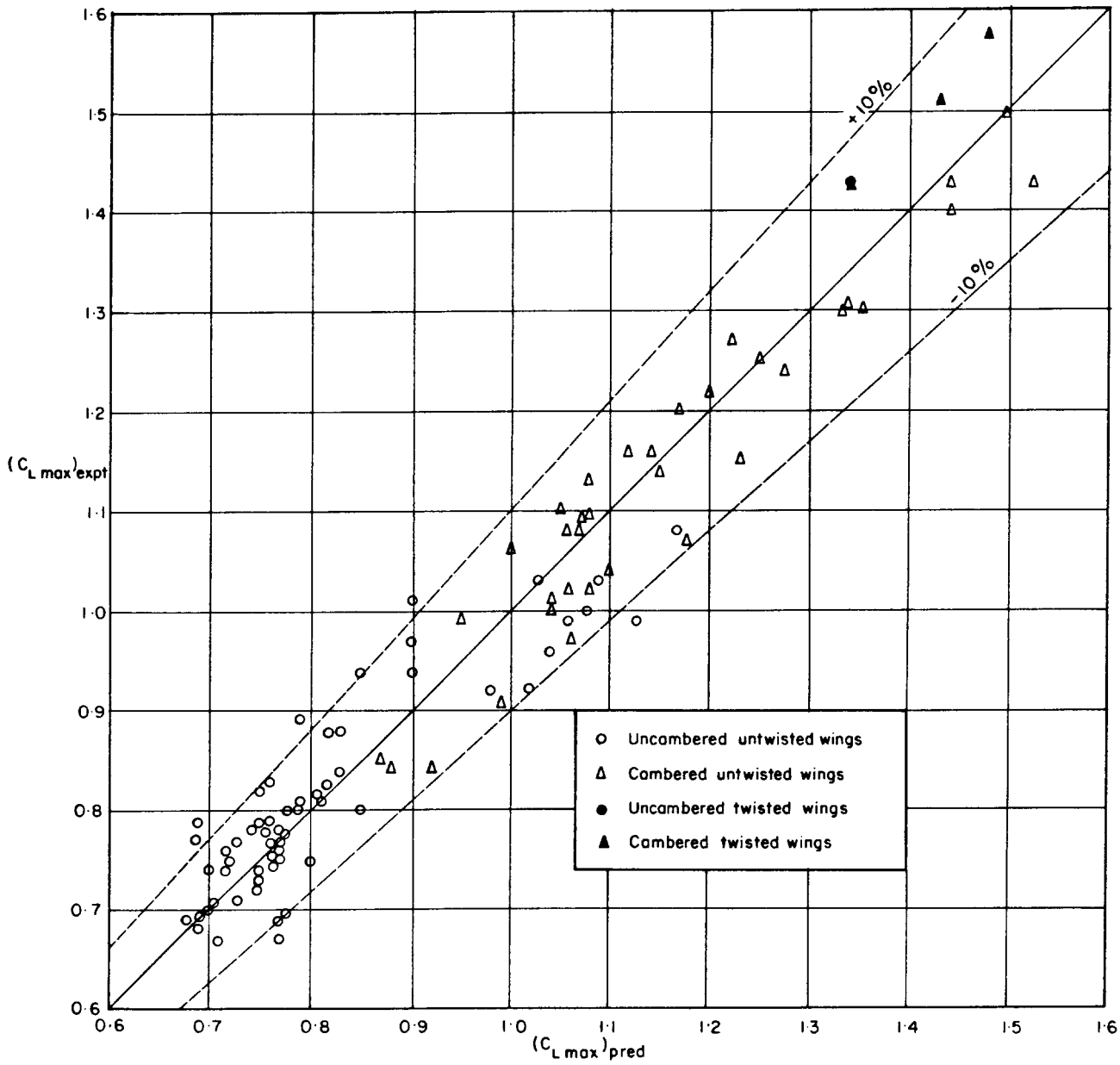

Sketch 7.2 Correlation for swept wings $10° < \Lambda_0 \leq 40°$

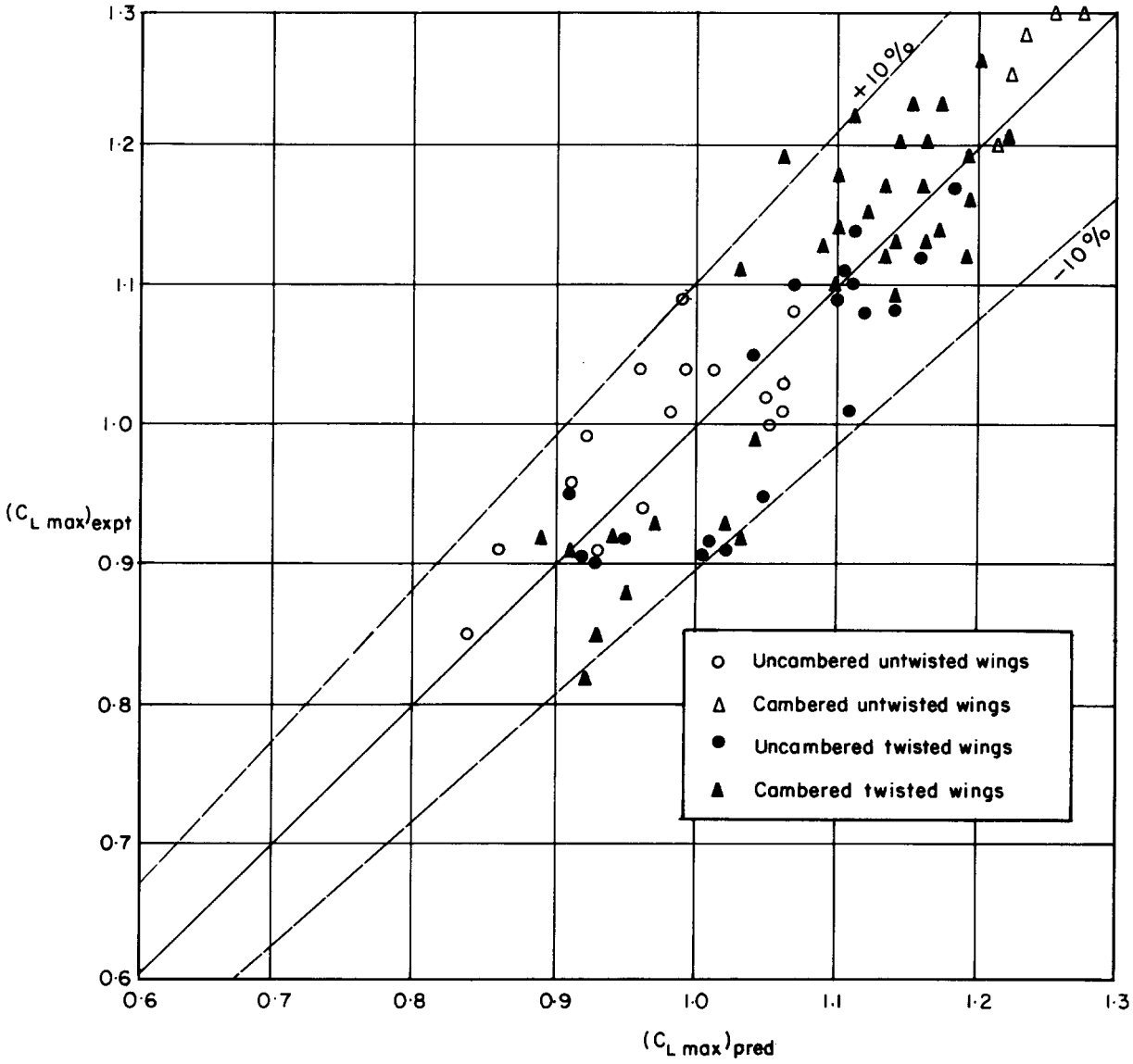

Sketch 7.3 Correlation for swept wings $40° < \Lambda_0 < 50°$

8. DERIVATION

The Derivation lists selected sources of information that have been used in the preparation of this Item.

1. ESDU — Slope of lift curve for two-dimensional flow. ESDU International, Item No. Aero W.01.01.05, 1955.

2. ESDU — The low-speed stalling characteristics of aerodynamically smooth aerofoils. ESDU International, Item No. 66034, 1966.

3. ESDU — Geometrical properties of cranked and straight tapered wing planforms. ESDU International, Item No. 76003, 1976.

4. ESDU — Method for the rapid estimation of spanwise loading of wings with camber and twist in subsonic attached flow. ESDU International, Item No. 83040, 1983.

5. ESDU — Aerofoil maximum lift coefficient for Mach numbers up to 0.4. ESDU International, Item No. 84026, 1984.

6. ESDU — Boundaries of linear characteristics of cambered and twisted wings at subcritical Mach numbers. ESDU International, Item No. 88030, 1988.

7. ANDERSON, R.F. — Determination of the characteristics of tapered wings. NACA Rep. 572, 1936.

8. SOULE, H.A. ANDERSON, R.F. — Design charts relating to the stalling of tapered wings. NACA Rep. 703, 1940.

9. SHORTAL, J.A. MAGGIN, B. — Effect of sweepback and aspect ratio on longitudinal stability characteristics of wings at low speeds. NACA tech. Note 1093, 1946.

10. NEELY, R.H. BOLLECH, T.V. WESTRICK, G.C. GRAHAM, R.R. — Experimental and calculated characteristics of several NACA 44 series wings with aspect ratios of 8, 10 and 12 and taper ratios of 2.5 and 3.5. NACA tech. Note 1270, 1947.

11. PROTERRA, A.G. — Aerodynamic characteristics of a 45 degree swept-back wing with aspect ratio of 3.5 and NACA 2S-50(05)-50(05) airfoil sections. NACA RM L7C11 (TIL 1623), 1947.

12. KOVEN, W. GRAHAM, R.R. — Wind-tunnel investigation of high-lift and stall-control devices on a 37 degree sweptback wing of aspect ratio 6 at high Reynolds numbers. NACA RM L8D29 (TIL 1907), 1948.

13. CAHILL, J.F. GOTTLIEB, S.M. — Low speed aerodynamic characteristics of a series of swept wings having NACA 65A006 airfoil sections. NACA RM L50F16 (TIL 2555), 1950.

14. SALMI, R.J. CARROS, R.J. — Longitudinal characteristics of two 47.7 degree sweptback wings with aspect ratios of 5.1 and 6 at Reynolds numbers up to 10×10^6. NACA RM L50A04 (TIL 2361), 1950.

15. DEMELE, F.A.
SUTTON, F.B.
The effects of increasing the leading edge radius and adding forward camber on the aerodynamic characteristics of a wing with 35 degrees of sweepback.
NACA RM A50K28a (TIL 2638), 1950.

16. TINLING, B.E.
KOLK, W.R.
The effects of Mach number and Reynolds number on the aerodynamic characteristics of several 12% thick wings having 35 degrees of sweepback and various amounts of camber.
NACA RM A50K27 (TIL 2629), 1951.

17. HARPER, J.H.
Wind-tunnel investigation of effects of various aerodynamic balance shapes and sweepback on control surface characteristics of semispan tail surfaces with NACA 0009, 0015, 66-009, 66(215)-014, and circular arc airfoil sections.
NACA tech. Note 2495, 1951.

18. GOODMAN, A.
Effects of wing position and horizontal-tail position on the static stability characteristics of models with unswept and 45 degree sweptback surfaces with some reference to mutual interference.
NACA tech. Note 2504, 1951.

19. DOBBS, J.B.
TINLING, B.E.
Summary of results of a wind-tunnel investigation of 9 related horizontal tails.
NACA RM A51G31a (TIL 2895), 1951.

20. FITZPATRICK, J.E.
SCHNEIDER, W.C.
Effects of Mach number variation between 0.07 and 0.34 and Reynolds number variation between 0.97×10^6 and 8.1×10^6 on the maximum lift coefficient of a wing of NACA 64-210 airfoil sections.
NACA tech. Note 2753, 1952.

21. JAQUET, B.M.
Effect of linear spanwise variations of twist and circular arc camber on low-speed static stability, rolling and yawing characteristics of a 45 degree sweptback wing of aspect ratio 4 and taper ratio 0.6.
NACA tech. Note 2775, 1952.

22. LOPEZ, A.E.
TINLING, B.E.
The effects of Reynolds number at Mach numbers up to 0.94 on the loading on a 35 degree sweptback wing having NACA 65_1-A012 streamwise section.
NACA RM A52B20 (TIL 3189), 1952.

23. SALMI, R.J.
Low-speed longitudinal aerodynamic characteristics of a twisted and cambered wing of 45 degrees sweepback and aspect ratio 8 with and without high-lift and stall-control devices and a fuselage at Reynolds numbers from 1.5×10^6 to 4.8×10^6.
NACA RM L52C11 (TIL 3192), 1952.

24. BOLTZ, F.W.
KOLBE, C.D.
The forces and pressure distribution at subsonic speeds on a cambered and twisted wing having 45 degrees of sweepback, an aspect ratio of 3, and a taper ratio of 0.5.
NACA RM A52D22 (TIL 3268), 1952.

25. EDWARDS, G.G.
TINLING, B.E.
ACKERMAN, A.C.
The longitudinal characteristics at Mach numbers up to 0.92 of a cambered and twisted wing having 40° of sweepback and an aspect-ratio of 10.
NACA RM A52F18 (TIL 3318), 1952.

26. JONES, G.W.
Investigation of the effects of variations in the Reynolds number between 0.4×10^6 and 3.0×10^6 on the low-speed aerodynamic characteristics of 3 low-aspect-ratio symmetrical wings with rectangular planforms.
NACA RM L52G18 (TIL 3128), 1952.

27. KIRK, F.N.
STAPLES, K.J.
A collection of low speed information from tests of wings without bodies.
RAE tech. Note Aero 2155, 1952.

28. GRAHAM, R.R.
JACQUES, W.A.
Wind-tunnel investigation of stall control by suction through a porous leading edge on a 37 degree sweptback wing of aspect ratio 6 at Reynolds numbers from 2.5×10^6 to 8.1×10^6.
NACA RM L52L05 (TIL 3656), 1953.

29. FOSTER, G.V.
MOLLENBERG, E.F.
WOODS, R.L.
Low-speed longitudinal characteristics of an unswept hexagonal wing with and without a fuselage and a horizontal tail located at various positions at Reynolds numbers from 2.8×10^6 to 7.6×10^6.
NACA RM L52L11b (TIL 3640), 1953.

30. TURNER, T.R.
Effects of rate of flap deflection on flap hinge moment and wing lift through the Mach number range from 0.32 to 0.87.
NACA RM L53E11 (TIL 3777), 1953.

31. HADAWAY, W.M.
Low-speed longitudinal characteristics of two unswept wings of hexagonal airfoil sections having aspect ratios of 2.5 and 4.0 with fuselage and with horizontal tail located at various vertical positions.
NACA RM L53H14a (TIL 3938), 1953.

32. SUTTON, F.B.
DICKSON, C.K.
A comparison of the longitudinal aerodynamic characteristics at Mach numbers up to 0.94 of sweptback wings having NACA 4 digit or NACA 64A thickness distributions.
NACA RM A54F18 (TIL 4335), 1954.

33. NELSON, H.
ALLEN, E.C.
KRUMM, W.J.
The transonic characteristics of 36 symmetrical wings of varying taper, aspect ratio and thickness as determined by the transonic bump technique.
NACA tech. Note 3529, 1955.

34. FURLONG, G.C.
McHUGH, J.G.
A summary and analysis of low speed longitudinal characteristics of swept wings at high Reynolds number.
NACA Rep. 1339, 1957.

35. GOULD, S.
A collection of low speed information from tests of wings without bodies.
RAE tech. Note Aero 2155(A), 1958.

36. BORE, C.L.
BOYD, A.T.
Estimation of maximum lift of swept wings at low Mach numbers. *J.R. aeronaut. Soc.*,Vol. 67, pp. 227-239, April 1963.

37. HARPER, C.W.
MAKI, R.L.
A review of the stall characteristics of swept wings.
NASA tech. Note D-2373, 1964.

38. van den BERG, B.
Reynolds number and Mach number effects on the maximum lift and the stalling characteristics of wings at low speeds.
NLR TR 69025 U, 1969.

39. McVEIGH, M.A.
KISIELOWSKI, E.
A design summary of stall characteristics for straight wing aircraft.
NASA CR-1646, 1971.

40. BENEPE, D.B.
Development of aerodynamic prediction methods of irregular planform wings.
NASA CR-3664, 1983.

9. EXAMPLE

Estimate the maximum lift coefficient for a wing with twist and with camber varying across the span for a Reynolds number $R_{\bar{c}} = 7\times10^6$ and $M = 0.3$. The wing has the following characteristics:

$$A = 8, \Lambda_{¼} = 25°, \lambda = 0.4 \ .$$

Streamwise root section NACA 63-012 with $x_{um}/c = 0.350, z_{um}/c = 0.0600$ and $\alpha_{0r} = 0, C_{L0r} = 0$.

Streamwise tip section NACA 63-412 with $x_{um}/c = 0.399$, $z_{um}/c = 0.0806$ and $\alpha_{0t} = –3.14°$ $C_{L0t} = 0.334$.

Camber varies linearly across the span.

Geometric twist, root to tip (δ_t), is –4.4° (*i.e.* leading edge down) and varies linearly across the span.

1. **Determine** *the required wing planform parameters*

$A, \Lambda_{¼}$ and λ are given, and so from the relationships for planform geometry given in Item No. 76003 (Derivation 3).

$$A\tan\Lambda_0 = A\tan\Lambda_{¼} + \left(\frac{1-\lambda}{1+\lambda}\right) = 3.7305 + 0.4286 = 4.159 \ ,$$

so that

$$\Lambda_0 = 27.47° \ .$$

Also,

$$A\tan\Lambda_{½} = A\tan\Lambda_{¼} - \left(\frac{1-\lambda}{1+\lambda}\right) = 3.7305 - 0.4286 = 3.302 \ ,$$

so that

$$\Lambda_{½} = 22.43° \ .$$

Finally

$$A\tan\Lambda_1 = A\tan\Lambda_{¼} - 3\left(\frac{1-\lambda}{1+\lambda}\right) = 3.7305 - 1.2857 = 2.445 \ ,$$

so that

$$\Lambda_1 = 17.00^\circ \ .$$

The wing taper parameter in Item No. 83040 (Derivation 4) is given by

$$\kappa = \frac{1+2\lambda}{3(1+\lambda)}$$

which, with $\lambda = 0.4$, gives

$$\kappa = (1+0.8)/(3\times 1.4) = 0.429 \ .$$

2. **Determine $\bar{\eta}$**

Since $M = 0.3$, $\beta A = 0.954\times 8.0 = 7.6$ and so Figure 4 of Item No. 83040 gives, with $A\tan\Lambda_{½} = 3.302$ and $\kappa = 0.429$,

$$\bar{\eta} = 0.4374 \, .$$

3. **Determine η_p**

From Figure 1, with $\bar{\eta} = 0.4374$ and $\lambda = 0.4$,

$$\eta_p = 0.69 \, .$$

4. **Determine μ_p**

From Figure 2, with $\bar{\eta} = 0.4374$ and $\lambda = 0.4$,

$$\mu_p = 1.15 \, .$$

5. **Determine $R_{cp}\cos^2\Lambda_0, \zeta_p$** *and, if necessary,* $\tan\tau_u\sec\Lambda_1$, *appropriate to* η_p

For $\lambda = 0.4$ and $\eta_p = 0.69$ the streamwise chord c_p at η_p is given by Equation (8.2) in Derivation 6 with $\Lambda_0 = 0$, *i.e.*

$$\begin{aligned} c_p/\bar{\bar{c}} &= \frac{3}{2}\left[\frac{1+\lambda}{1+\lambda+\lambda^2}\right](1-\eta_p+\lambda\eta_p) \\ &= 1.3461\times 0.586 \\ &= 0.7888 \, . \end{aligned}$$

The Reynolds number at η_p is given by:

$$R_{cp} = R_{\bar{\bar{c}}} \times c_p/\bar{\bar{c}}$$
$$= 7 \times 10^6 \times 0.7888$$
$$= 5.522 \times 10^6 .$$

Hence $R_{cp}\cos^2\Lambda_0 = 5.522 \times 10^6 \times 0.7873 .$

$$= 4.347 \times 10^6 .$$

From Table 5.1 of Item No. 66034 $z_{u1.25}/c = 0.0152$ for the root (NACA 63-012 at $\eta = 0$) section, and 0.0185 for the tip (NACA 63-412 at $\eta = 1$) section. Interpolation for $\eta_p = 0.69$ gives a NACA 63-(2.76)12 section, for which, by similar interpolation in $z_{u1.25}/c$,

$$(z_{u1.25}/c)_p = 0.0175 .$$

Hence $\zeta_p = (z_{u1.25}/c)_p \sec\Lambda_0 = 0.0175 \times 1.127$

$$= 0.0197 .$$

As $\zeta_p > 0.017$ it is necessary to evaluate C_{Lm} for a trailing-edge stall, which requires $\tan\tau_u$. Interpolation for $\eta_p = 0.69$ in the values of x_{um}/c and z_{um}/c given for the root $(\eta = 0)$ and tip $(\eta = 1)$ sections gives, for the section at η_p,

$$x_{um}/c = 0.384 \text{ and } z_{um}/c = 0.0742 .$$

With these values, Equation (6.2) gives

$$\tan\tau_u = (z_{um}/c)/(1 - x_{um}/c)$$
$$= 0.0742/0.616$$
$$= 0.1205 .$$

Hence $\tan\tau_u \sec\Lambda_1 = 0.1205 \times 1.0457$

$$= 0.1260 .$$

6. **Determine** C_{L0} *for section at* η_p

Linear interpolation between the given values of $C_{L0} = 0$ for the root and 0.334 for the tip gives the value at η_p as

$$C_{L0} = 0.230 .$$

7. **Determine** C_{Lm} *for* η_p

For $\tan\tau_u \sec\Lambda_1 = 0.126$ and $R_{cp}\cos^2\Lambda_0 = 4.35 \times 10^6$ the increment in maximum lift coefficient, ΔC_L, from Figure 2 of Item No. 84026 is

$$\Delta C_L = 1.39 .$$

Based on Equation (2.1) in Item No. 84026 for $M = 0$,

$$C_{Lm} = \Delta C_L + C_{L0}\sec\Lambda_0$$

which, for the section at η_p, gives

$$C_{Lm} = 1.39 + 0.230 \times 1.127 = 1.649 .$$

8. **Determine** C_{Lmax} *for the swept wing*

From Equation (6.9)

$$C_{Lmax} = C_{Lm}/\mu_p + \Delta C_{LM} + \Delta C_{LR} + \Delta C_{L\Lambda} + \Delta C_{LT} .$$

For $M = 0.3$ and $\Lambda_0 = 27.47°, \Delta C_{LM}$ is obtained using Figure 3 where, for $M\cos\Lambda_0 = 0.3 \times 0.8872 = 0.266$ and $\zeta_p = 0.0197$,

$$\Delta C_{LM}/\cos^4\Lambda_0 = -0.19$$

and hence

$$\Delta C_{LM} = -0.19 \times 0.62$$
$$= -0.118 .$$

Since $\Lambda_0 < 37°$, Figure 4 gives

$$\Delta C_{LR} = 0 .$$

For $\Lambda_0 = 27.47°$ and $\zeta_p = 0.0197$, Figure 5b gives

$$\Delta C_{L\Lambda} = -0.030 .$$

Finally, since both the geometric and camber-dependent twist vary linearly across the span, the effective tip twist from Equation (6.5) is

$$\delta_{et} = \delta_t + \alpha_{0r} - \alpha_{0t}$$
$$= -4.4 + 0 - (-3.14)$$
$$= -1.26° .$$

From Figure 6, with $\lambda = 0.4, A = 8, \Lambda_{½} = 22.43°$ (*i.e.* $\tan\Lambda_{½} = 0.413$), interpolation gives

$$\Delta C_{LT} = \frac{\Delta C_{LT}}{\delta_{et}} \times \delta_{et}$$
$$= -0.0016 \times -1.26$$
$$= 0.002 .$$

Hence

$$C_{Lmax} = 1.649/1.15 + (-0.118) + 0 + (-0.030) + 0.002$$
$$= 1.29 .$$

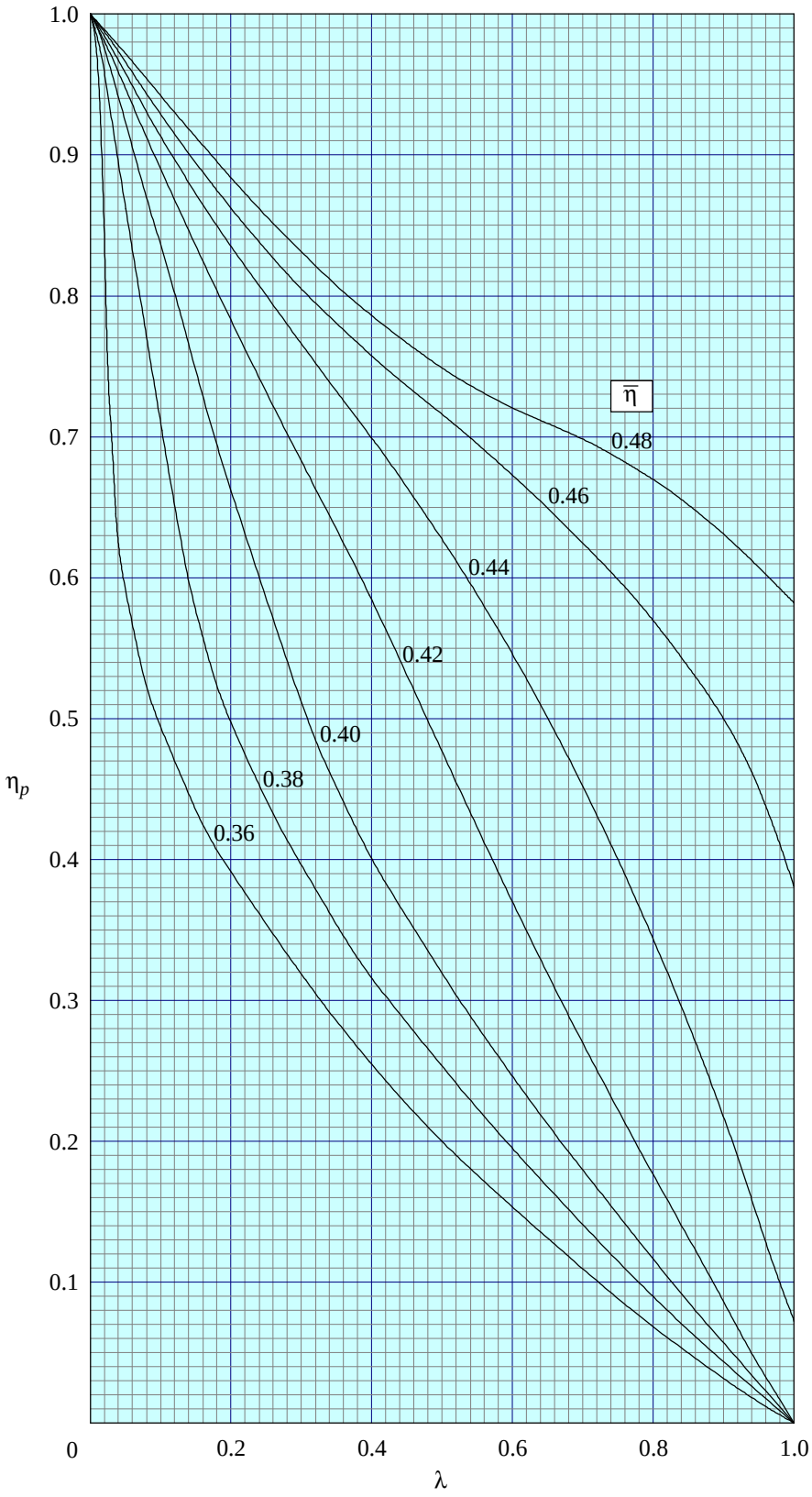

FIGURE 1 VARIATION OF η_p WITH λ AND $\bar{\eta}$

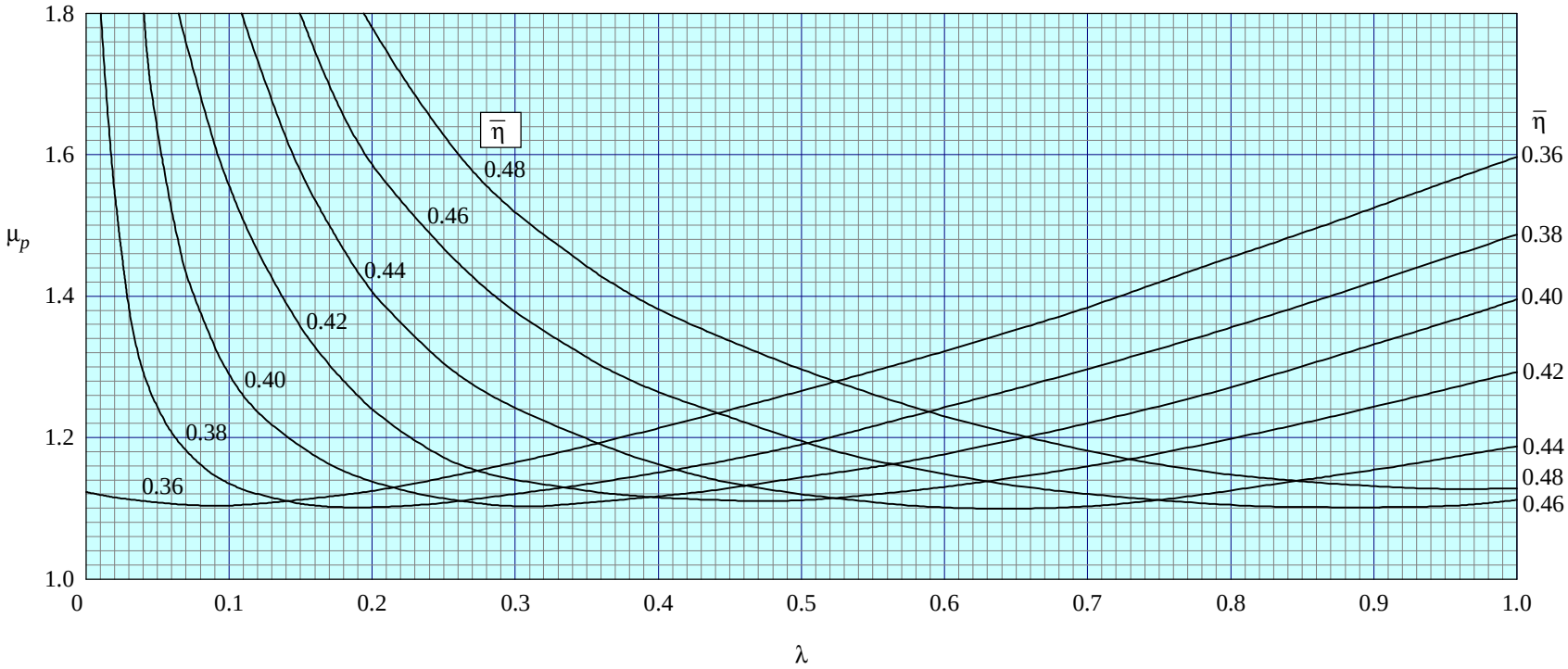

FIGURE 2 VARIATION OF μ_p WITH λ AND $\bar{\eta}$

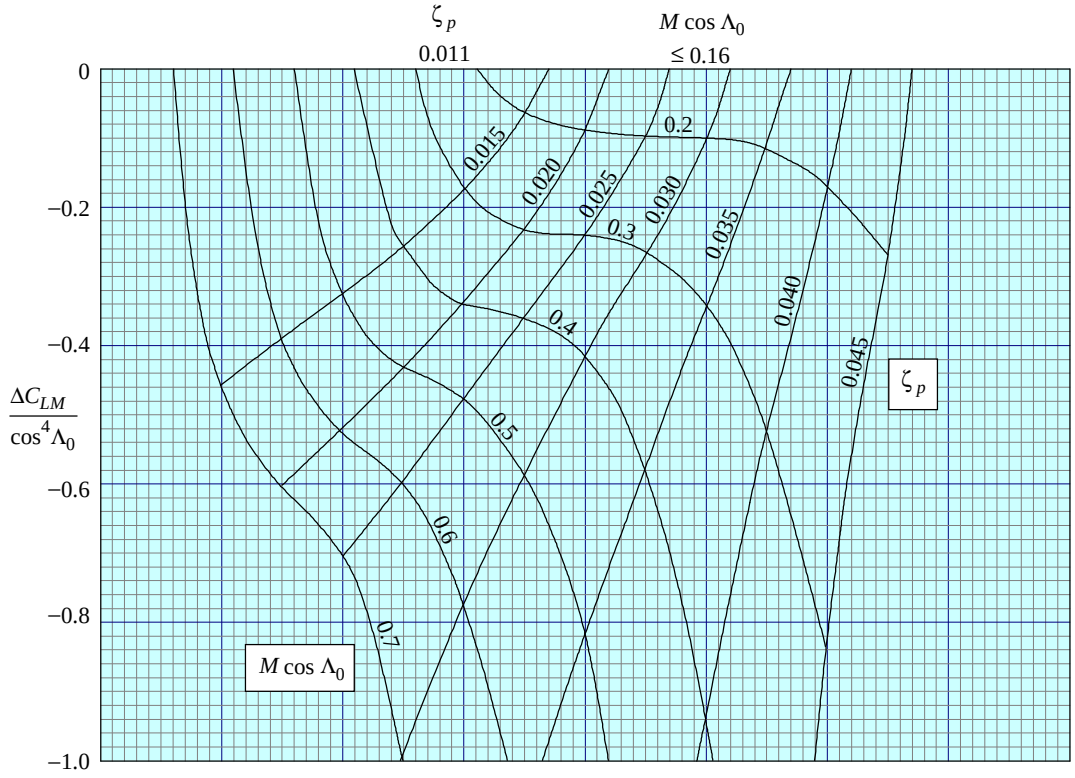

FIGURE 3 INCREMENT ΔC_{LM} DUE TO MACH NUMBER

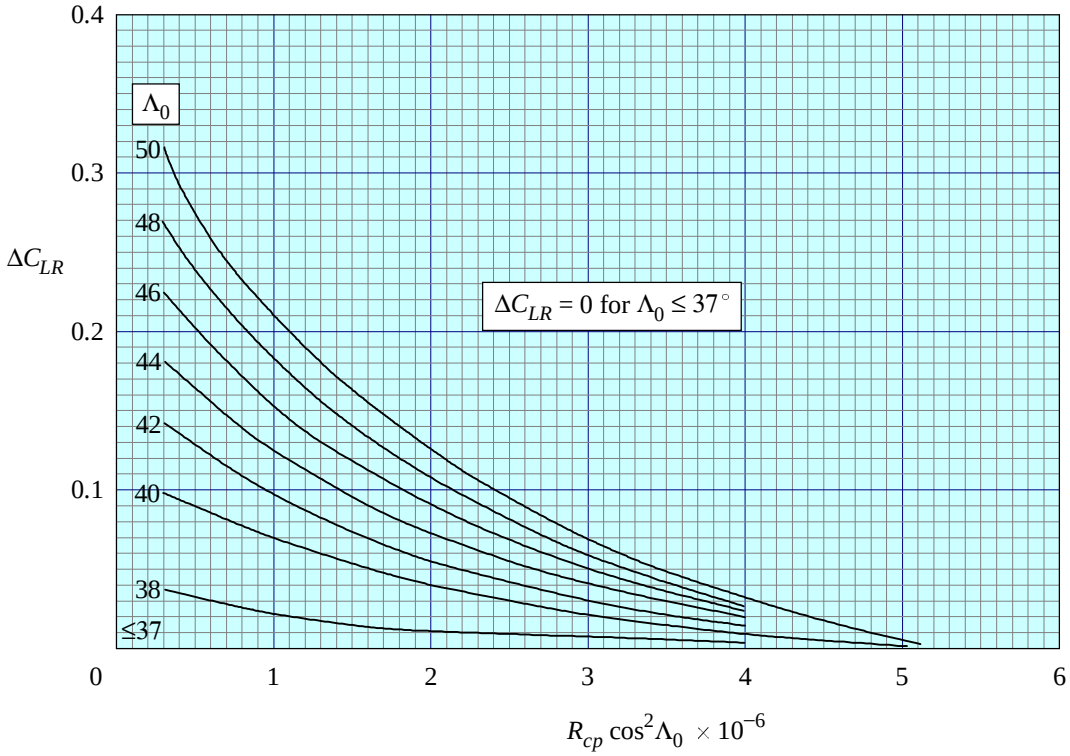

FIGURE 4 INCREMENT ΔC_{LR} DUE TO REYNOLDS NUMBER

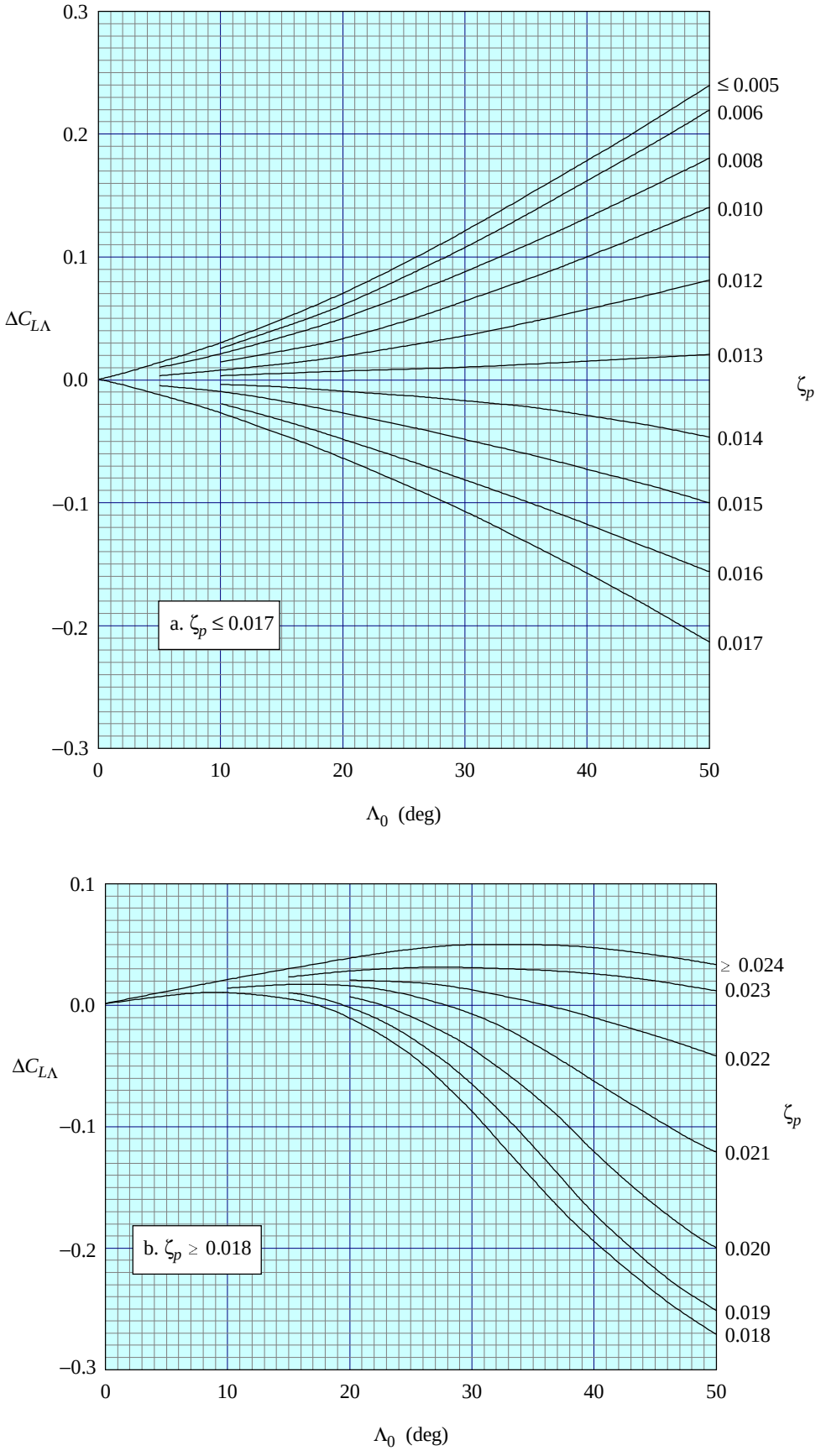

FIGURE 5 INCREMENT $\Delta C_{L\Lambda}$ FOR SWEPT WINGS

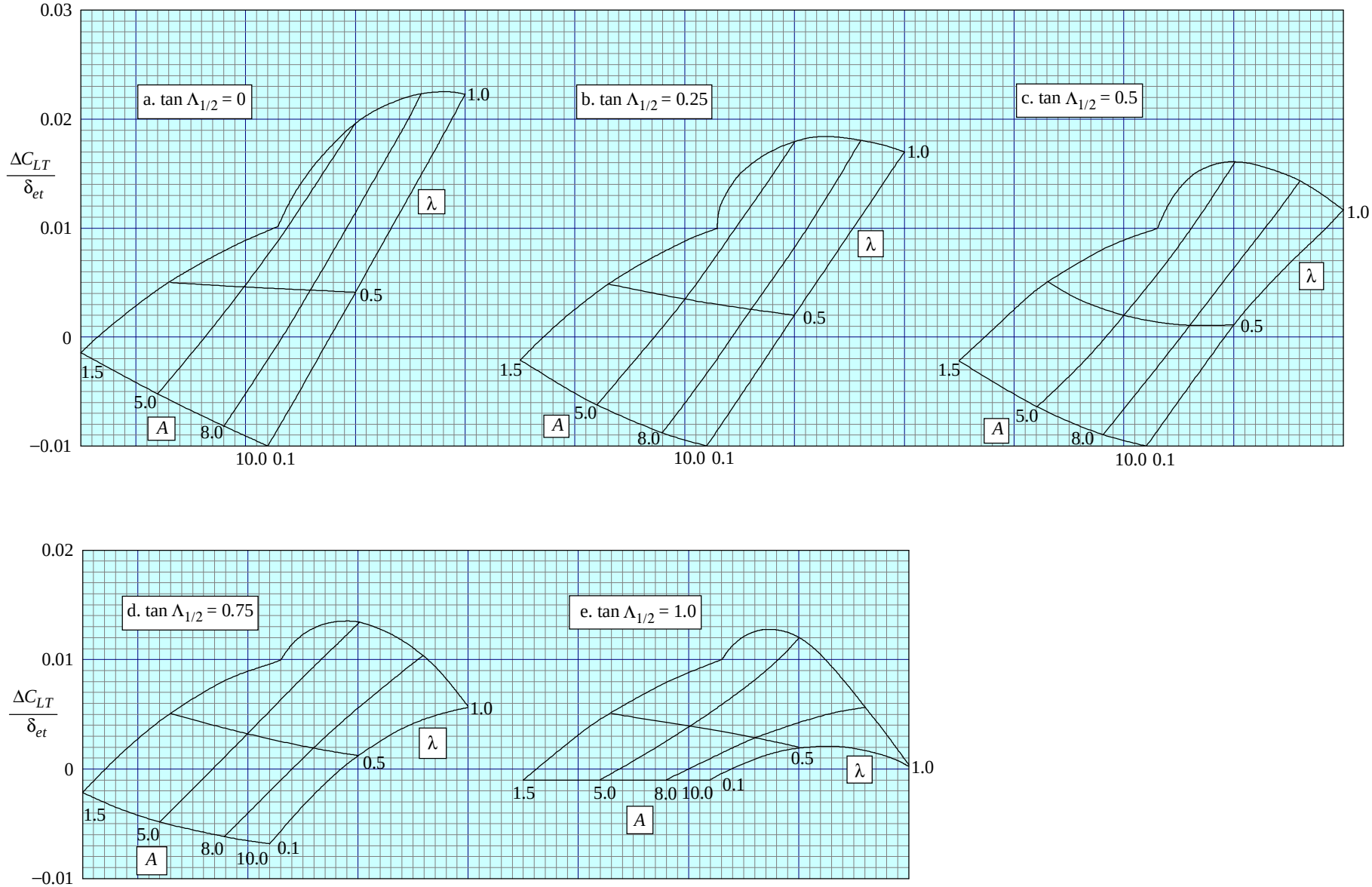

FIGURE 6 INCREMENT DUE TO TWIST, ΔC_{LT}

THE PREPARATION OF THIS DATA ITEM

The work on this particular Data Item was monitored and guided by the Aerodynamics Committee, which first met in 1942 and now has the following membership:

Chairman

Mr H.C. Garner	–	Independent

Vice-Chairman

Mr P.K. Jones	–	British Aerospace (Commercial Aircraft) Ltd, Woodford

Members

Mr G.E. Bean*	–	Boeing Aerospace Company, Seattle, Wash., USA
Dr N.T. Birch	–	Roll-Royce plc, Derby
Mr K. Burgin	–	Southampton University
Dr T.J. Cummings	–	Short Brothers plc
Mr J.R.J. Dovey	–	Independent
Mr L. Elmeland*	–	Saab-Scania, Linköping, Sweden
Dr J.W. Flower	–	Independent
Dr K.P. Garry	–	Cranfield Institute of Technology
Mr P.G.C. Herring	–	Sowerby Research Centre, Bristol
Mr R. Jordan	–	Aircraft Research Association
Mr J.H. Krause*	–	Northrop Corporation, Hawthorne, Calif., USA
Mr J.R.C. Pedersen	–	Independent
Mr R. Sanderson	–	Messerschmitt-Bölkow-Blohm GmbH, Bremen, Germany
Mr A.E. Sewell*	–	McDonnell Douglas, Long beach, Calif., USA
Mr M.R. Smith	–	British Aerospace (Commercial Aircraft) Ltd, Bristol
Miss J. Willaume	–	Aérospatiale, Toulouse, France

* Corresponding Member

The technical work in the assessment of the available information and the construction and subsequent development of the Data Item was carried out under contract to ESDU by Mr J.R.J. Dovey.